

## Accepted Manuscript

## International Journal of Modern Physics D

Article Title: Hubble Inflation in Randall-Sundrum Type II model

Author(s): Habib Abedi, Amir M. Abbassi, Sebastian Bahamonde

DOI: 10.1142/S0218271820500376

Received: 30 September 2019

Accepted: 23 February 2020

To be cited as: Habib Abedi, Amir M. Abbassi, Sebastian Bahamonde, Hubble Inflation in Randall-Sundrum Type II model, *International Journal of Modern Physics D*, doi: 10.1142/S0218271820500376

Link to final version: <https://doi.org/10.1142/S0218271820500376>

This is an unedited version of the accepted manuscript scheduled for publication. It has been uploaded in advance for the benefit of our customers. The manuscript will be copyedited, typeset and proofread before it is released in the final form. As a result, the published copy may differ from the unedited version. Readers should obtain the final version from the above link when it is published. The authors are responsible for the content of this Accepted Article.

February 23, 2020 10:59 WSPC/INSTRUCTION FILE Abedi

International Journal of Modern Physics D  
 © World Scientific Publishing Company

## Hubble Inflation in Randall-Sundrum Type II model

Habib Abedi

*Department of Physics, University of Tehran,  
 North Kargar Avenue, 14399-55961 Tehran, Iran.  
 h.abedi@ut.ac.ir*

Amir M. Abbassi

*Department of Physics, University of Tehran,  
 North Kargar Avenue, 14399-55961 Tehran, Iran.  
 amabasi@khayam.ut.ac.ir*

Sebastian Bahamonde

*Laboratory of Theoretical Physics, Institute of Physics, University of Tartu,  
 W. Ostwaldi 1, 50411 Tartu, Estonia.  
 Department of Mathematics, University College London,  
 Gower Street, London, WC1E 6BT, United Kingdom.  
 sbahamonde@ucl.ac.uk  
 sebastian.beltran.14@ucl.ac.uk*

Received Day Month Year

Revised Day Month Year

We study a braneworld Randall-Sundrum type II (RSII) model using the Hamilton-Jacobi formalism. We extend the standard inflationary parameters and the flow equations for this braneworld scenario. We investigate the conditions that reduce the infinite number of flow equations into a finite number and confirm that by considering that one of the inflationary parameters vanishes, the Hubble expansion rate gets a polynomial form in both General Relativity and in the high-energy regime of RSII. We also show that if one sets this inflationary parameter to a constant value, the model features a non-polynomial form of the Hubble expansion rate. The form of the Hubble parameter in this case is different in General Relativity and RSII. Next, we consider a single-scalar field model with a Hubble expansion rate behaving as  $H \propto \phi^n$  and show that compared to GR, the RSII model has a smaller tensor-to-scalar ratio and larger spectral index for  $n > 1$ . Therefore, RSII model leads to better predictions than General Relativity.

**Keywords:** Inflation; Braneworld scenario ; Flow equations

**PACS numbers:**

### 1. Introduction

Inflation was proposed in order to solve some problems in cosmology such as the horizon and the flatness problems. It also provide a quantum mechanical origin for anisotropies observed in the cosmic microwave background and primordial density

2 *H. Abedi, A.M.Abbassi, S.Bahamonde*

perturbations that form large-scale structures.

The Randall-Sundrum type II (RSII) model was first proposed as an attempt to solve the hierarchy problem in the standard model of particle physics. The large noncompact extra dimension decreases the scale of gravity to weak scale and solves the hierarchy problem. The developments in string theory have increased the interest in such models. In RSII,<sup>1</sup> it is assumed that matter fields are trapped on a 3-brane embedded into a 5-dimensional spacetime with a  $Z_2$  symmetry. In this model, gravity can propagate into the bulk. For a complete review on RSII model see Refs. 2–13. One of most important features of RSII is the modification of the Friedmann equation, which now reads as

$$H^2 = \frac{8\pi}{3M_4^2} \rho \left( 1 + \frac{\rho}{2\mu} \right), \quad (1)$$

where  $H = \dot{a}/a$  is the Hubble expansion rate,  $\rho$  is the energy density of the matter fields confined on the brane and  $\mu = 6M_5^6/M_4^2$  is an intrinsic tension on the brane. Here, the constants  $M_4$  and  $M_5$  are the 4D and 5D Planck masses, respectively. The above equation is obtained by considering a spatially flat Friedmann-Robertson-Walker (FRW) spacetime on the brane. In the limit  $\mu \rightarrow \infty$ , we recover the standard Friedmann equation. The quadratic term in the above Friedmann equation (1) decays as  $a^{-8}$  during the radiation dominated epoch, therefore, it can be neglected in this epoch. However, during inflation, it might result in considerable effects and it cannot be ignored in general. On the other hand, The modified expansion law of RSII, modifies common phenomena in cosmology, e.g. gravitino production,<sup>14,15</sup> baryogenesis,<sup>15–17</sup> dark matter relic abundance<sup>18–23</sup> and etc.

The Hubble expansion rate  $H$  is a fundamental quantity in the Hamilton-Jacobi approach that can be written as a function of multiple scalar fields. Then, inflation is described by a tower of flow parameters depending on the Hubble parameter (see Refs. 24,25 and references therein). Then, by truncating these flow equations, one can describe the dynamics of inflation in an exact form. The multiple scalar-field inflation in this context was studied in Ref. 24. For the high-energy limit of the RSII model, the Hamilton-Jacobi formalism with a single field was studied in Refs. 26–28 and its flow equations in Refs. 29,30. In Refs. 24,31, the authors found conditions to ensure that all the higher order inflationary parameters vanish. Then, infinite number of flow equations would reduce to a finite number of first order differential equations. If we set a parameter (at some order) to zero, the model is equivalent to the case where we consider a polynomial Hubble expansion rate. Although the polynomial model is convenient to study inflation in many cases, it would be interesting to study more general classes of models. Setting some parameters equal to zero is not the only way to obtain a finite number of equations for the inflationary parameters. For instance, in Ref. 32 was shown that if one inflationary parameter is constant, e.g.  $^{(m)}\lambda = \text{const.}$ , the equations at the  $m$ -th and higher orders become algebraic and then, the higher order parameters can be expressed in terms of the lower order ones. On the other hand, if one sets one of the inflationary parameters to be a

constant, this leads to a non-polynomial Hubble expansion rate. The flow equations can be used to study the stability of different cosmological solutions. As an example, in this paper we consider flow equations with  $^{(2)}\lambda = 0$  and  $^{(2)}\lambda = \text{const.}$ , and show that for  $^{(2)}\lambda \neq 0$ , the fixed point is the only past time attractor. The equations and parameters used in this work are reduced to the GR case in the low-energy limit.

In general, inflationary observables (such as the tensor-to-scalar ratio or the spectral index) are modified in the RSII model compared to General Relativity (GR). Although braneworld inflation models with a single power-law potential  $V \propto \phi^n$  are now ruled out by recent observational constraints, they have been widely studied. Different power-law parameters  $n$  have been studied in Refs. 11, 12, 33, showing that in general, braneworld inflationary models are in disfavour with respect to GR. Surprisingly, using our approach, we find that RSII models can explain inflation in a better agreement with observations than GR. The aim of this work is to study RSII model in the Hamilton-Jacobi formalism and compare it to GR. This paper is organized as follows:

- In Sec. 2, we consider a flat FRW background spacetime and generalize the multiple fields parameters and flow equations defined in Ref. 24 for the RSII model. While the modified parameters and flow equations are not the same as those in GR, we confirm that the truncation condition is the same as in GR and the potential would be restricted to a polynomial inflationary field. We then focus on the high- and low-energy regimes separately. In each case, we consider that one of the inflationary parameters is a constant. In the low-energy limit regime, we get the same potential studied in Ref. 32; however, in high-energy regimes, we get models that cannot be studied only by truncating the equations.
- Sec. 3 is devoted to show how different inflationary observables are modified by considering a RSII model. Such effects also exist in single scalar field models in a slow-roll regime, therefore, as a simple and important example, we investigate a single potential with a Hubble expansion rate being  $H \propto \phi^n$  with general  $n$ . After this, we study different values of  $n$  to analyse how inflationary observables change. We confirm that if we consider the Hubble parameter as a fundamental quantity, RSII models will result in decreasing (increasing) the tensor-to-scalar ratio for  $n > 1$  ( $n < 1$ ).

Throughout this work we use  $i, j, k \dots = 1, 2, 3, \dots$  for scalar fields  $\phi^i$  and Greek indices  $\mu, \nu, \dots = 1, 2, 3, 4$  for spacetime indices. We set the reduced Planck mass to  $M_4 = 1.2 \times 10^{19} \text{GeV}$ .

## 2. General flow equations for multiple scalar fields

Let us consider a set of multiple scalar fields confined on the brane denoted by  $\phi_i$ , with  $i = 1, \dots, N$ , in a flat FRW background  $ds^2 = -dt^2 + a(t)^2(dx^2 + dy^2 + dz^2)$ .

4 *H. Abedi, A.M. Abbassi, S. Bahamonde*

The total energy of the scalar fields is given by

$$\rho = \frac{1}{2} \dot{\phi}^i \dot{\phi}_i + V(\phi^i), \quad (2)$$

where  $V(\phi^i)$  is a general potential and dots denote derivatives with respect to the cosmic time  $t$ . The Klein-Gordon equation for each scalar field can be written as

$$\ddot{\phi}^i + 3H\dot{\phi}^i + \frac{\partial V(\phi^j)}{\partial \phi^i} = 0. \quad (3)$$

Using Eq. (1), the energy density can be written as a function of the scalar fields, namely

$$\rho = \mu \sqrt{\frac{3M_4^2}{4\pi\mu} H^2 + 1} - \mu. \quad (4)$$

By taking time derivatives in Eqs. (2) and (4) and then by using the Klein-Gordon equation (3), one finds

$$\dot{\phi}^i = -\frac{M_4^2}{4\pi} \frac{H_{,i}}{\sqrt{\frac{3M_4^2}{4\pi\mu} H^2 + 1}}, \quad (5)$$

where  $H_{,i} := \partial H / \partial \phi^i$ . Eq. (5) can be also obtained by doing similar calculations as it was done in Refs. 24, 31, 35. In low-energy regime ( $\mu \rightarrow \infty$ ), we recover the same standard equation reported in Ref. 35 (see Eq. (2.14a)), which reads

$$\dot{\phi}^i = -\frac{M_4^2}{4\pi} H^{,i}, \quad (6)$$

whereas in the high-energy limit ( $\mu \ll 1$ ), Eq. (5) is reduced to

$$\dot{\phi}^i = -\sqrt{\frac{\mu M_4^2}{12\pi}} \frac{H^{,i}}{H}. \quad (7)$$

By replacing Eqs. (4) and (5) into (2), one finds that the potential behaves as

$$V(\phi^i) = \mu \sqrt{\frac{3M_4^2}{4\pi\mu} H^2 + 1} - \frac{1}{2} \left( \frac{M_4^2}{4\pi} \right)^2 \frac{H_{,i} H^{,i}}{\frac{3M_4^2}{4\pi\mu} H^2 + 1} - \mu. \quad (8)$$

Inflationary parameters are defined with the Hubble expansion rate and its derivatives with respect to the scalar fields. Then, the flow equations which depend on the inflationary parameters form an infinite set of ordinary differential equations. Let us use the standard definition of the slow-roll inflationary parameter  $\epsilon$  given by

$$\epsilon = -\frac{\dot{H}}{H^2}, \quad (9)$$

where one can notice that an accelerated expansion  $\ddot{a}/a = H^2(1-\epsilon) > 0$  is obtained when  $\epsilon < 1$ . Using Eq. (5), we find that this parameter becomes

$$\epsilon = \frac{M_4^2}{4\pi} \frac{H_{,i} H^{,i}}{H^2 F^2}, \quad (10)$$

where for simplicity we have defined the function

$$F(H) = \left( \frac{3M_4^2}{4\pi\mu} H^2 + 1 \right)^{1/4}. \quad (11)$$

It is then possible to rewrite the slow-roll parameter  $\epsilon$  as

$$\epsilon = \epsilon_i \epsilon^i, \quad (12)$$

where we have defined

$$\epsilon_i := \sqrt{\frac{M_4^2}{4\pi}} \frac{H_{,i}}{HF}. \quad (13)$$

The evolution of the parameter  $\epsilon_i$  can be then written using the above definitions, namely

$$\frac{d\epsilon_i}{dN} = \lambda_{ij} \epsilon^j - \epsilon_i \epsilon \gamma(x), \quad (14)$$

where  $N = \log(a)$  is the number of e-foldings, and  $d/dN = -d/Hdt$ . In the above equation, we have also introduced the following quantities:

$$\gamma(x) := \frac{\frac{3}{2}x^2 + 1}{x^2 + 1}, \quad (15)$$

$$x := \sqrt{\frac{3M_4^2}{4\pi\mu}} H, \quad (16)$$

and

$$\lambda_{ij} := \frac{M_4^2}{4\pi} \frac{H_{,ij}}{HF^2}, \quad (17)$$

and we have used  $dH/dN = -\epsilon H$ . We can further compute the evolution of  $\lambda_{ij}$  which gives us

$$\frac{d\lambda_{ij}}{dN} = {}^{(2)}\lambda_{ij} - \lambda_{ij} \epsilon \beta(x), \quad (18)$$

where

$$\beta(x) := \frac{2x^2 + 1}{x^2 + 1} \quad (19)$$

and

$${}^{(2)}\lambda_{ij} := \left( \frac{M_4^2}{4\pi} \right)^2 \left( \frac{1}{HF^2} \right)^2 H_{,ijk} H^{,k}. \quad (20)$$

In the same way, we can generalize this result by defining higher order inflationary parameters as follows:

$${}^{(m)}\lambda_{\nu_0 \nu_1} := \left( \frac{M_4^2}{4\pi} \right)^m \left( \frac{1}{HF^2} \right)^m H_{,\nu_0 \dots \nu_m} \prod_{i=2}^m H^{,\nu_i}, \quad m \geq 2. \quad (21)$$

6 *H. Abedi, A.M.Abbassi, S.Bahamonde*

Then, the flow evolution of these higher order parameters  $^{(m)}\lambda_{\nu_0 \nu_1}$  can be expressed as

$$\frac{d^{(m)}\lambda_{ij}}{dN} = {}^{(m+1)}\lambda_{ij} + {}^{(m)}W_{ij} - m {}^{(m)}\lambda_{ij} \epsilon \beta(x), \quad (22)$$

where

$${}^{(m)}W_{\nu_0 \nu_1} := \left( \frac{M_4^2}{4\pi} \frac{1}{HF^2} \right)^{m+1} H_{,\nu_0 \dots \nu_m} \sum_{k=2, I=1}^m \prod_{j=2, j \neq k}^m H_I H^{I\nu_k} H^{,\nu_j}. \quad (23)$$

It should be noted that Eq. (22) is only valid for  $m \geq 2$ . Eqs. (14), (18) and (22) form an infinite hierarchy of differential equations. These equations are a generalisation of the standard flow equations due to the existence of the functions  $\gamma$  and  $\beta$ . By taking the case  $^{(m)}\lambda_{\nu_0 \nu_1} = 0 = {}^{(m)}W_{\nu_0 \nu_1}$  for all  $\nu_0$  and  $\nu_1$ , and then by choosing a specific  $m$ , all higher order parameters vanish. Therefore, the condition for truncating the flow equation to a closed form is

$$H_{,\nu_0 \dots \nu_m} = 0, \quad (24)$$

which gives the Hubble parameter  $H(\phi^i)$  behaving as a polynomial form described by,<sup>24,31</sup>

$$H = \sum_{a,b,c,\dots} A_{a,b,c,\dots} (\phi^1)^a (\phi^2)^b (\phi^3)^c \dots, \quad (25)$$

where sums go from  $a+b+c+\dots=0$  to  $a+b+c+\dots=m$ . Eq. (22) does not take any assumption on the potential. However, truncating these equations is equivalent to restricting the models considered. In the low-energy regime ( $\gamma = \beta = 1$ ), we recover the flow equations obtained in Ref. 24. In a single scalar field model, the flow equations are reduced to the following standard flow equations,<sup>36,37</sup>

$$\frac{d\epsilon}{dN} = \epsilon [\omega + 2\epsilon(2 - \gamma(x))], \quad (26)$$

$$\frac{d\omega}{dN} = -(4 + \beta(x))\epsilon\sigma - 4\epsilon^2 [\beta(x) + 2(2 - \gamma(x))] + 2^{(2)}\lambda,$$

$$\frac{d^{(m)}\lambda}{dN} = {}^{(m)}\lambda \left\{ \frac{m-1}{2}\sigma + \epsilon [m(2 - \beta(x)) - 2] \right\} + {}^{(m+1)}\lambda, \quad m \geq 2, \quad (27)$$

where  $\omega := 2\lambda - 4\epsilon$  was defined and, we have used the fact that  $^{(m)}W = {}^{(m)}\lambda \lambda(m-1)$  in a single scalar field inflationary model.

Fig. 1 shows the flow of the parameters  $\epsilon$  and  $\lambda$  for the condition  $^{(2)}\lambda = 0$ , that is equivalent as having  $\partial^3 H / \partial \phi^3 = 0$ , for the following system:

$$\frac{d\epsilon}{dN} = 2\epsilon [\lambda - \epsilon \gamma(x)], \quad (28)$$

$$\frac{d\lambda}{dN} = {}^{(2)}\lambda - \lambda \epsilon \beta(x). \quad (29)$$

In this figure, blue areas show the accelerating regime whereas arrows indicate the inflationary direction. Both low- and high-energy regimes result in a similar flow.

Notice that the values of  $\epsilon$  and  $\lambda$  affect the scalar spectral index  $n_s$  and tensor-to-scalar ratio  $r$  at the horizon exit; after this period,  $\epsilon$  and  $\lambda$  do not affect the value of  $n_s$  and  $r$ . From Fig. 1, one can notice that some trajectories do not cross the line  $\epsilon = 1$  since in this case, inflation should be ended by another physical process. For small  $\epsilon$  and  $\lambda$ , as it is in GR at the horizon exit, the line  $\epsilon = \lambda/2$  coincides with  $n_s = 1$ . Then,  $\epsilon > \lambda/2$  indicates that  $n_s < 1$  and on the contrary,  $\epsilon < \lambda/2$  results in  $n_s > 1$ . In the high-energy regime of RSII,  $n_s = 1$  is equivalent as having  $\epsilon = \lambda/3$ . The fixed critical point for both high- and low-energy regimes with  $^{(2)}\lambda = 0$  is  $\epsilon = 0$  and  $\lambda = \text{const.}$ . Then, the stability matrix of the system at this critical point for both high- and low-energy regimes becomes

$$\mathcal{J}|_{\epsilon=0} = \lambda \begin{pmatrix} 2 & 0 \\ -1 & 0 \end{pmatrix}. \quad (30)$$

One can find that the above stability matrix has two eigenvalues, 0 and  $2\lambda$ . Since one of eigenvalues vanishes, the point is non-hyperbolic and linear stability theory fails to study its stability properties. One can use center manifold theory to determine the behavior of trajectories around this point (see Ref. 38 for a review about dynamical systems and also how to use center manifold theory). The line  $\epsilon = 0$  with  $\lambda > 0$  attracts some of trajectories starting at  $\epsilon = 0 = \lambda$ . However, the line  $\epsilon = 0$  with  $\lambda < 0$  repels some other trajectories (see Fig. 1). This behavior can also be concluded from the sign of the eigenvalue  $2\lambda$ . By constraining  $r$  and  $n_s$ , one can set observational constraints for the values of the parameters at the horizon crossing. Fig. 2 shows the flow of  $\epsilon$  and  $\lambda$  for a single field inflationary model for GR and RSII, considering the truncation condition  $^{(2)}\lambda = 0$ .

The above analysis is restricted to a polynomial Hubble expansion rate. However, one can truncate the flow equations without setting the higher order flow parameters equal to zero.<sup>32</sup> Considering  $^{(m)}\lambda = \text{const.}$ , one can express the higher parameters in term of the lower parameters, i.e.

$$^{(m+1)}\lambda = ^{(m)}\lambda [m\epsilon\beta - (m-1)\lambda]. \quad (31)$$

Then, infinite number of equations would be reduced to a set of  $m$  ordinary differential equations. As an example, let us consider the case  $\epsilon = \text{const.}$ . In the low-energy regime we find that the Hubble parameter becomes

$$H(\phi) = H_0 \exp\left(\pm \sqrt{\frac{4\pi\epsilon}{M_4^2}} \phi\right), \quad (32)$$

that is equivalent to the following potential

$$V(\phi) = V_0 \exp\left(\pm \sqrt{\frac{16\pi\epsilon}{M_4^2}} \phi\right), \quad (33)$$

where  $V_0 = M_4^2 H_0 (3 - \epsilon)/8\pi$ . On the other hand, in the high-energy regime



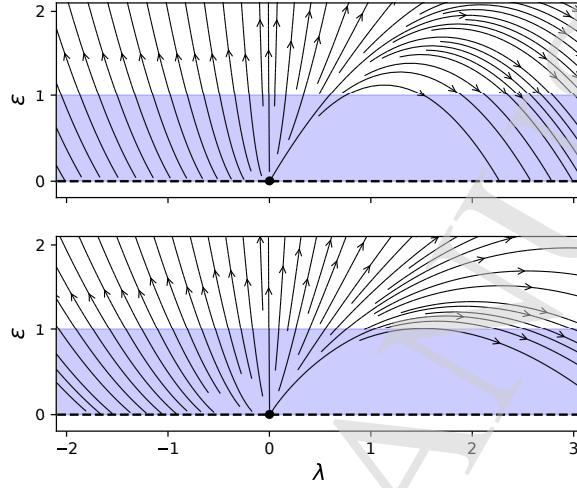


Fig. 1. Flow of  $\epsilon$  and  $\lambda$  considering the truncation condition  $^{(2)}\lambda = 0$  in a single field inflationary model. The upper figure describes GR (low-energy limit of RSII) while the lower figure shows RSII in the high-energy limit. The blue area represents the accelerating regime.

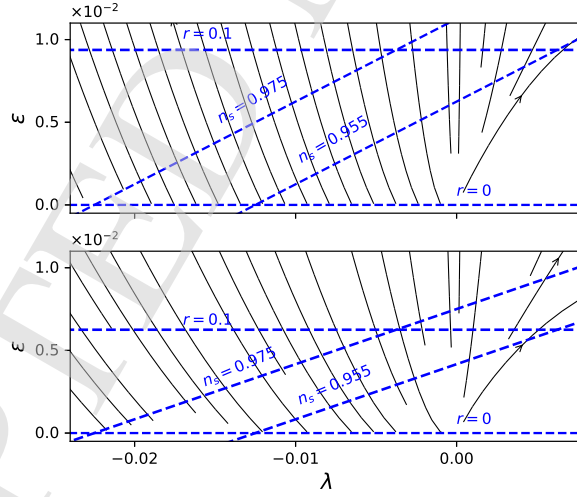


Fig. 2. Flow of  $\epsilon$  and  $\lambda$  considering the truncation condition  $^{(2)}\lambda = 0$  in a single field inflationary model. The upper figure describes GR (low-energy limit of RSII) while the lower figure shows RSII in high-energy limit. Notice that  $\epsilon$  and  $\lambda$  should be in the region confined by dashed lines at horizon crossing. Dashed lines describes  $r = 0, 0.1$  and  $n_s = 0.955, 0.975$ .

with  $\epsilon = \text{const.}$ , the Hubble parameter reads as follows

$$H(\phi) = \frac{H_0}{\left(1 \pm 2\sqrt{\frac{3\pi\epsilon^2}{M_4^2\mu H_0^2}}\phi\right)^2}, \quad (34)$$

with the related potential being

$$V(\phi) = \frac{V_0}{\left(1 \pm 2\sqrt{\frac{3\pi\epsilon^2}{M_4^2\mu H_0^2}}\phi\right)^2}, \quad (35)$$

where  $V_0 = \sqrt{\frac{M_4^2\mu}{3\pi}}\left(\frac{3}{2}H_0 - \frac{\epsilon}{H_0}\right)$ . The Hubble parameter in the form of Eqs. (32) and (34) cannot be obtained from setting the flow parameters equal to zero. With  $\epsilon = 0$ , Eqs. (32) and (34) lead to  $H = H_0$ . For  ${}^{(2)}\lambda = \text{const.}$ , the low-energy fixed point is  $\epsilon = \lambda = \sqrt{{}^{(2)}\lambda}$  whereas, in the high-energy regime, we find  $\epsilon = \sqrt{{}^{(2)}\lambda}/3$  and  $\lambda = \sqrt{3}{}^{(2)}\lambda/4$ . While the condition  ${}^{(2)}\lambda = \text{const.}$  can be analytically solved in the low-energy regime for different signs of  ${}^{(2)}\lambda$ ,<sup>32</sup> in the high-energy case, there are not any analytical solutions except for the specific case when  ${}^{(2)}\lambda = 0$ . The Jacobian matrix (stability matrix) evaluated at the fixed

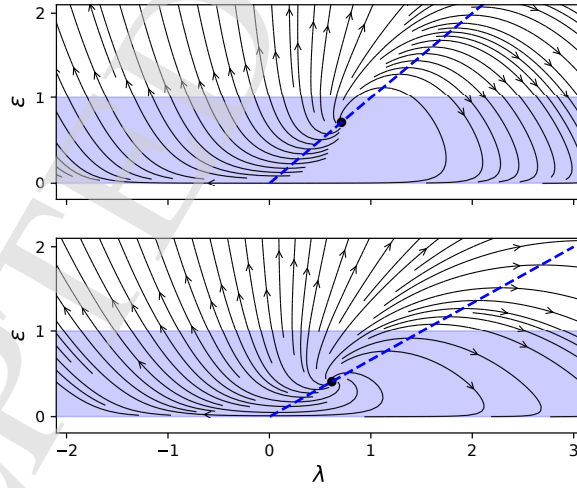


Fig. 3. Flow of parameters  $\epsilon$  and  $\lambda$  with the condition  ${}^{(2)}\lambda = 0.5$ . Blue dashed lines show the fixed point for different values of  ${}^{(2)}\lambda$ .

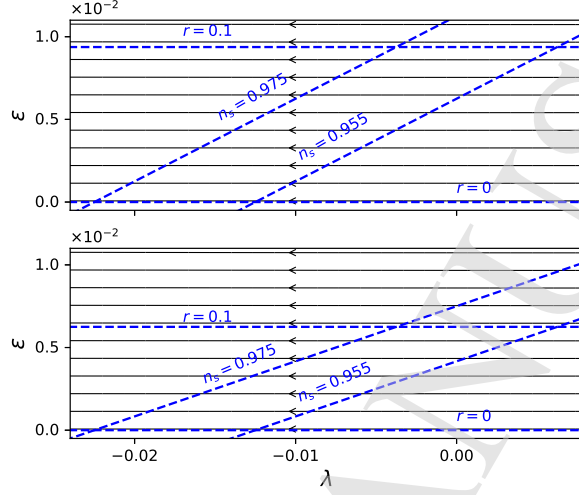


Fig. 4. Flow of parameters  $\epsilon$  and  $\lambda$  with the condition  $^{(2)}\lambda = 0.5$ . Observational constraint set constraints on these parameters at the horizon crossing. Dashed lines show the same region as in Fig. 2.

point  $\epsilon = \sqrt{^{(2)}\lambda/3}$  and  $\lambda = \sqrt{3^{(2)}\lambda/4}$  is

$$\mathcal{J}|_{\text{GR}} = \sqrt{^{(2)}\lambda} \begin{pmatrix} -2 & 2 \\ -1 & -1 \end{pmatrix}, \quad (36)$$

$$\mathcal{J}|_{\text{RSII high-energy}} = \sqrt{3^{(2)}\lambda} \begin{pmatrix} -1 & \frac{2}{3} \\ -1 & -\frac{2}{3} \end{pmatrix}. \quad (37)$$

Their eigenvalues are  $\sqrt{^{(2)}\lambda}(-3 \pm \sqrt{7}i)/2$  and  $\sqrt{3^{(2)}\lambda}(-5 \pm \sqrt{23}i)/6$ , respectively. In both cases, the eigenvalues are complex with negative real part; therefore, this point is an unstable spiral in both limits. This fixed point is the only past time attractor. Figs 3 and 4 show the phase space diagram for both low- and high-energy regimes with  $^{(2)}\lambda = 0.5$ . Notice that the fixed points for both limits (GR and high-energy of RSII) are above the lines  $\epsilon = \lambda/2$  and  $\epsilon = \lambda/3$ , respectively. Comparing Fig. 1 and 3, one notices that the flow lines significantly are different in small  $\epsilon$  for  $^{(2)}\lambda = 0$  and  $^{(2)}\lambda \neq 0$ .

In general, the fixed point for  $^{(m)}\lambda = \text{const.}$  is

$$\begin{aligned} \lambda &= \epsilon \gamma(x), \\ ^{(m)}\lambda &= ^{(m-1)}\lambda \epsilon [(m-1)\beta(x) - (m-2)\gamma(x)]. \end{aligned} \quad (38)$$

For constant  $\gamma$  and  $\beta$ ,  $\epsilon$  is also a constant and  $^{(m)}\lambda \propto \epsilon^m$ .

### 3. Slow-roll single field inflation

In single-field inflation, the curvature perturbation  $\zeta$  is conserved on super-horizon scales. On the other hand, in multiple-field inflation,  $\zeta$  can change outside the horizon. In this section we are going to discuss some consequences of using the Hubble function as a fundamental quantity; therefore, we restrict our attention to the single field case. We also assume that the slow-roll approximation is valid during inflation.

When one is considering a slow-roll regime, it is common to define inflationary parameters using the potential and its derivatives. In this regime, the parameters  $\epsilon$  and  $\lambda$  become

$$\epsilon = \frac{M_4^2}{16\pi} \frac{V'^2}{V^2} \frac{1 + \frac{V}{\mu}}{\left(1 + \frac{V}{2\mu}\right)^2}, \quad (39)$$

$$\lambda = \eta - \frac{\epsilon}{\left(1 + \frac{V}{\mu}\right)^2}, \quad (40)$$

where  $\eta$  is the standard inflationary slow-roll parameter,<sup>39</sup> expressed as

$$\eta = \frac{M_4^2}{8\pi} \frac{V''}{V \left(1 + \frac{V}{2\mu}\right)} \quad (41)$$

with primes denoting derivatives with respect to the scalar field  $\phi$ . In the low-energy regime,  $\mu \gg V$ , and the inflationary parameters are reduced to

$$\epsilon = \frac{M_4^2}{16\pi} \frac{V'^2}{V^2}, \quad (42)$$

$$\eta = \frac{M_4^2}{8\pi} \frac{V''}{V}, \quad (43)$$

$$\eta = \lambda + \epsilon. \quad (44)$$

Another important parameter in inflation is the number of e-foldings  $N$  which is defined as,

$$N = \int_{t_{\text{end}}}^t H dt, \quad (45)$$

where  $t_{\text{end}}$  is the end of inflation determined by

$$\epsilon(\phi_{\text{end}}^i) = 1. \quad (46)$$

One can rewrite  $N$  as an integration on scalar fields

$$N = -\frac{4\pi}{M_4^2} \int_{\phi_{\text{end}}^i}^{\phi^i} H F^2 A_i d\phi^i, \quad (47)$$

where  $A = A(\phi^i)$ , and

$$A_i H^{,i} = 1. \quad (48)$$

12 *H. Abedi, A.M.Abbassi, S.Bahamonde*

In a single-field model,  $A = 1/H'$  and

$$N = -\frac{4\pi}{M_4^2} \int_{\phi_{\text{end}}}^{\phi} \frac{HF^2}{H'} d\phi. \quad (49)$$

Then, the number of e-foldings in the slow-roll regime yields

$$N = -\frac{8\pi}{M_4^2} \int_{\phi_{\text{end}}}^{\phi} \frac{V}{V'} \left(1 + \frac{V}{2\mu}\right) d\phi, \quad (50)$$

where  $A = 1/V'$ . In the low-energy limit, Eq. (50) gives the common GR expression for the number of e-foldings.

The curvature perturbation for a single scalar field is given by

$$\zeta = -\frac{H}{\dot{\rho}} \delta\rho = -\frac{H}{\dot{\phi}} \delta\phi. \quad (51)$$

On large scales, the perturbation of the scalar field is the same as it is in the standard case based in GR,  $\delta\phi = H/2\pi$ , therefore, we get that the power spectra behaves as

$$\mathcal{P}_{\zeta} = \left(\frac{H}{\dot{\phi}}\right)^2 \left(\frac{H}{2\pi}\right)^2, \quad (52)$$

and in slow-roll regime, it becomes

$$\mathcal{P}_{\zeta} = \frac{9}{4\pi^2} \frac{H^6}{V'^2}. \quad (53)$$

The spectral tilt and its running get the following forms<sup>39</sup>

$$n_s - 1 := \frac{d \ln \mathcal{P}_{\zeta}}{d \ln k} = 2\eta - 6\epsilon, \quad (54)$$

$$\frac{dn_s}{d \ln k} = \frac{M_4^2}{4\pi} \frac{V'}{V} \frac{1}{1 + \frac{V}{2\mu}} \left(3 \frac{\partial \epsilon}{\partial \phi} - \frac{\partial \eta}{\partial \phi}\right). \quad (55)$$

Tensorial perturbations are more involved in braneworld inflationary models since the graviton can propagate into the bulk, and the amplitude of the tensorial perturbations would be different than its standard form as in GR. This mean that the power spectrum of tensorial perturbations is no longer proportional to  $H^2$ . The power spectrum of tensorial perturbations in RSII was obtained in Ref. 40 and is given by

$$\mathcal{P}_t = 8 \left(\frac{H}{2\pi}\right)^2 \mathcal{A}^2(x), \quad (56)$$

where

$$\mathcal{A}^2(x) := \left[ \sqrt{1+x^2} - x^2 \ln \left( \frac{1}{x} + \sqrt{1 + \frac{1}{x^2}} \right) \right]^{-1} \quad (57)$$

and  $x$  is defined in Eq. (16). In addition, the tensor-to-scalar ratio is given by

$$r = \frac{M_4^2}{\pi} \left(\frac{V'}{V}\right)^2 \frac{\mathcal{A}^2(x)}{\left(1 + \frac{V}{2\mu}\right)^2}. \quad (58)$$

In the low-energy regime ( $H \ll \mu$ ), we have  $\mathcal{A}(x) \approx 1$ , and on the contrary, in the high-energy regime ( $H \gg \mu$ ), we have  $\mathcal{A}(x) \approx \sqrt{3x/2}$ . Hereafter, we consider a special power-law form of the Hubble parameter  $H = \alpha\phi^n$ , where  $n$  and  $\alpha$  are constants. In the low-energy regime, the equations are reduced to the standard GR case. In this regime, the scalar field at the horizon crossing and at the end of inflation is

$$\phi_* = \sqrt{\frac{M_4^2}{4\pi} n(2N + n)}, \quad (59)$$

$$\phi_{\text{end}} = \sqrt{\frac{M_4^2}{4\pi} n}, \quad (60)$$

respectively. In this limit, using the power spectrum of scalar perturbations, we get

$$\alpha = \frac{M_4^2}{2} \sqrt{\mathcal{P}_\zeta} \left( \frac{4\pi}{M_4^2} \right)^{(n+1)/2} \frac{n}{[n(2N + n)]^{(n+1)/2}}. \quad (61)$$

We can also compute another important inflationary observables, such as

$$n_s = 1 - \frac{2(n+1)}{2N + n}, \quad (62)$$

$$r = \frac{16n}{2N + n}, \quad (63)$$

$$\frac{dn_s}{d \ln k} = -\frac{4(n+1)}{(2N + n)^2}. \quad (64)$$

Considering a high-energy braneworld,  $V/\mu \gg 1$ , we get that

$$H^2 = \frac{4\pi}{3M_4^2\mu} V^2. \quad (65)$$

The scalar field at horizon crossing and the end of inflation behaves respectively as,

$$\phi_* = \left\{ \sqrt{\frac{M_4^2\mu}{12\pi}} \frac{n}{\alpha} [(n+2)N + n] \right\}^{1/(n+2)}, \quad (66)$$

$$\phi_{\text{end}} = \left( \sqrt{\frac{M_4^2\mu}{12\pi}} \frac{n^2}{\alpha} \right)^{1/(n+2)}. \quad (67)$$

Then, from the power spectrum of scalar perturbations we get

$$\alpha = \left( \frac{3}{n^2\pi M_4^2 \mathcal{P}_\zeta} \right)^{-(n+2)/6} \left\{ \sqrt{\frac{M_4^2}{12\pi}} n [(n+2)N + n] \right\}^{-(2n+1)/3} \mu^{-(n-1)/6}. \quad (68)$$

Fig. 5 depicts the behaviour of  $\alpha$  versus  $M_5$  for the  $H = \alpha\phi^2$  case at different e-foldings and assuming a power spectrum equal to

$$\mathcal{P}_\zeta(k) = (2.22 \pm 0.16) \times 10^{-9}, \quad (69)$$

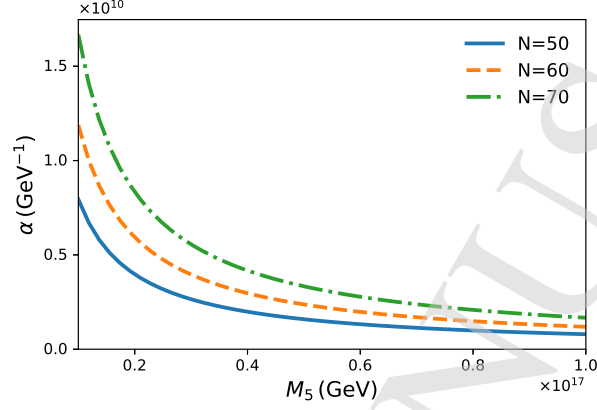


Fig. 5.  $\alpha$  vs.  $M_5$  for  $H = \alpha\phi^2$  and different numbers of e-folding  $N = 50, 60, 70$ .

with a pivot scale of  $k_0 = 0.002 \text{Mpc}^{-1}$ .<sup>41</sup> For general  $n$ , the other observables are:

$$n_s = 1 - \frac{2(2n+1)}{(n+2)N+n}, \quad (70)$$

$$r = \frac{24n}{(n+2)N+n}, \quad (71)$$

$$\frac{dn_s}{d \ln k} = -\frac{2(n+1)(2n+3)}{n^2 [(n+2)N+n]^2}. \quad (72)$$

Fig. 6 shows the tensor-to-scalar ratio vs. spectral index for different values of  $n$  in both the high- and low-energy regimes. In this figure we have considered  $N = 50, 60, 70$ . The bound  $N \leq 75$  on the number of e-folds was found in Ref. 42 for braneworld scenarios. The contours show the  $1\sigma$  ( $2\sigma$ ) confidence level obtained from Planck 2018, Bicep/Keck 2014 and the baryon acoustic oscillations (BAO) data.<sup>41</sup> For  $n > 1$  ( $n < 1$ ), the tensor-to-scalar ratio  $r$  decreases (increases); and the primordial tilt  $n_s$  increases (decreases). Therefore, considering the high-energy limit of RSII, analytical results for  $n > 1$  become closer to the observational region. Fig. 7 shows running of the spectral index  $dn_s/d \ln k$  vs. primordial tilt  $n_s$  for low- and high-energy limit of a braneworld model. As one can see from the figure, the running of the spectral index decreases for  $n > 1$ . We have also plotted the spectral index, tensor-to-scalar ratio and running of spectral index vs. number of e-folds in Figs. 8, 9 and 10. The gray band in Fig. 8 corresponds to 1- and 2- $\sigma$  for TT+lowP+lensing data.<sup>41</sup> Considering the strong regime of RSII not only increase the possible number of e-folds, but also push the lines toward the gray band.

#### 4. Conclusions

In this paper, we have studied inflation in braneworld RSII. We derived the general flow equations for the inflationary parameters in the presence of multiple scalar fields

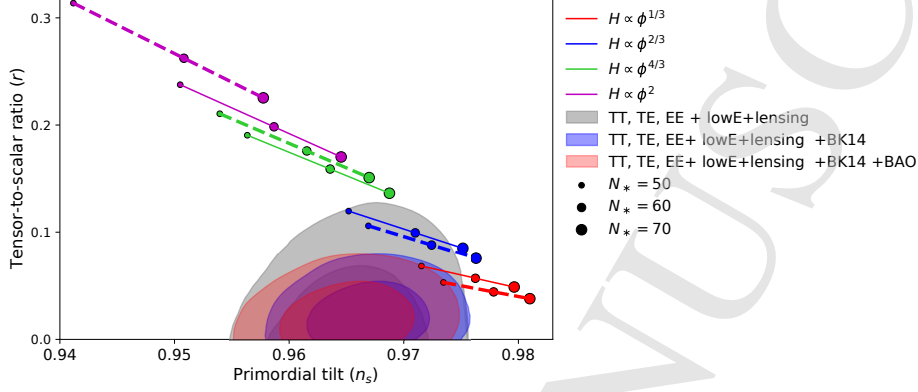


Fig. 6. Tensor-to-scalar ratio  $r$  vs. spectral index  $n_s$  for  $H = \alpha\phi^n$  in low-energy (dashed lines) and high-energy (solid lines) limit. The circles indicate  $N = 50, 60, 70$ .

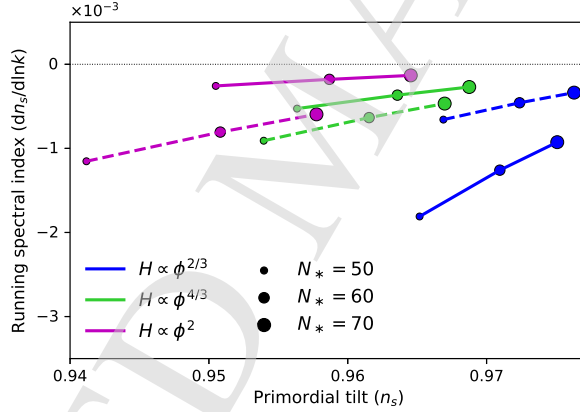


Fig. 7. Running spectral index vs. spectral index for  $H = \alpha\phi^n$  in low energy limit (dashed lines) and high-energy limit (solid lines). We have used  $N = 50, 60, 70$ .

and we found that the truncation condition used for the inflationary parameters is the same as the standard one considered in inflation based on GR (see Eq. (24)). If we consider that one of the inflationary parameters is a constant, then, the number of equations for the inflationary parameters becomes finite in both high- and low-energy regime. In this case, a new form of the Hubble expansion rate  $H$  is obtained. It is important to mention that this form cannot be found by just truncating the flow equations. The condition  $^{(m)}\lambda = \text{const.}$  leads to a nonlinear equation and hence, this equation can only be solved analytically for some small values of  $m$ . We have also shown analytically that by considering the Hubble expansion rate as a fundamental quantity, and a braneworld scenario with  $H \propto \phi^n$ , the tensor-to-scalar ratio is decreased for  $n > 1$ , that makes it more consistent with observational constraints obtained from Planck 2018 (see Fig. 6). This result differs from previous results such



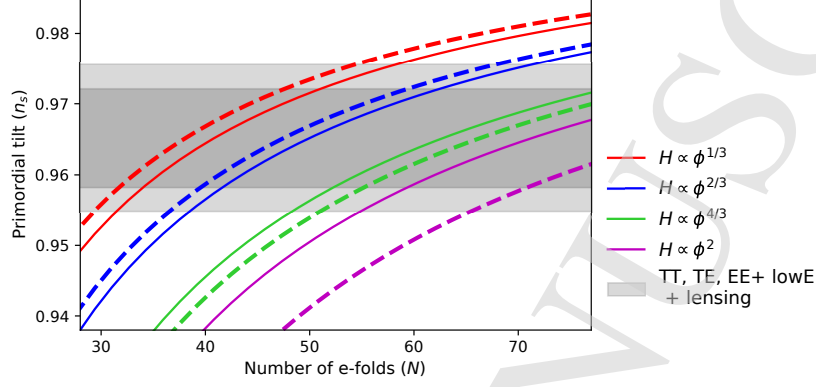


Fig. 8. Primordial tilt  $n_s$  vs. number of e-folds for various values of  $n$ , in low-energy limit (dashed lines) and high-energy limit (solid lines).

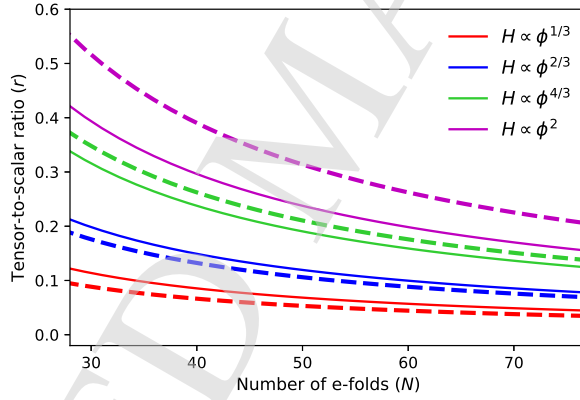


Fig. 9. Tensor-to-scalar ratio  $r$  vs. number of e-folds for various values of  $n$ , in low-energy limit (dashed lines) and high-energy limit (solid lines).

as Ref. 12 where the authors found that RSII was in disfavour comparable to GR. The main difference between our result and previous works is that we employed the Hamilton-Jacobi approach with the Hubble expansion rate being the fundamental quantity.

## References

1. L. Randall and R. Sundrum, *An Alternative to compactification*, *Phys. Rev. Lett.* **83**, 4690 (1999), [[hep-th/9906064](#)].
2. R. Maartens and K. Koyama, *Brane-World Gravity*, *Living Rev. Rel.* **13**, 5 (2010), [[arXiv:1004.3962 \[hep-th\]](#)].
3. D. Langlois, *Brane cosmology: An Introduction*, *Prog. Theor. Phys. Suppl.* **148**, 181 (2003), [[hep-th/0209261](#)].

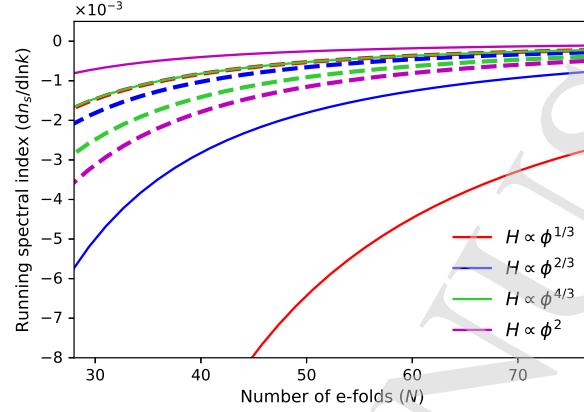


Fig. 10. Running of spectral index  $dn_s/d \ln k$  vs. number of e-folds for various values of  $n$ , in low-energy limit (dashed lines) and high-energy limit (solid lines).

4. P. Binetruy, C. Deffayet and D. Langlois, *Nonconventional cosmology from a brane universe*, *Nucl. Phys. B* **565**, 269 (2000), [[hep-th/9905012](#)].
5. C. Csaki, M. Graesser, C. F. Kolda and J. Terning, *Cosmology of one extra dimension with localized gravity*, *Phys. Lett. B* **462**, 34 (1999), [[hep-ph/9906513](#)].
6. J. M. Cline, C. Grojean and G. Servant, *Cosmological expansion in the presence of extra dimensions*, *Phys. Rev. Lett.* **83**, 4245 (1999), [[hep-ph/9906523](#)].
7. T. Shiromizu, K. i. Maeda and M. Sasaki, *The Einstein equation on the 3-brane world*, *Phys. Rev. D* **62**, 024012 (2000), [[gr-qc/9910076](#)].
8. P. Binetruy, C. Deffayet, U. Ellwanger and D. Langlois, *Brane cosmological evolution in a bulk with cosmological constant*, *Phys. Lett. B* **477**, 285 (2000), [[hep-th/9910219](#)].
9. D. Ida, *Brane world cosmology*, *JHEP* **0009**, 014 (2000), [[gr-qc/9912002](#)].
10. S. Mukohyama, T. Shiromizu and K. i. Maeda, *Global structure of exact cosmological solutions in the brane world*, *Phys. Rev. D* **62**, 024028 (2000), Erratum: [*Phys. Rev. D* **63**, 029901 (2001)], [[hep-th/9912287](#)].
11. N. Okada and S. Okada, *Simple brane-world inflationary models: an update*, *Int. J. Mod. Phys. B* **31**, no. 14n15, 1650078 (2016), [[arXiv:1504.00683 \[hep-ph\]](#)].
12. M. R. Gangopadhyay and G. J. Mathews, *Constraints on Brane-World Inflation from the CMB Power Spectrum: Revisited*, *JCAP* **1803**, no. 03, 028 (2018), [[arXiv:1611.05123 \[astro-ph.CO\]](#)].
13. R. Herrera, *Reconstructing braneworld inflation*, *AIP Conf. Proc.* **562**, 3 (2001), [[arXiv:1901.04607 \[gr-qc\]](#)].
14. N. M. C. Santos, *Gravitino production in the Randall-Sundrum II braneworld cosmology*, [hep-ph/0702200](#).
15. W. Abdallah, D. Delepine and S. Khalil, *TeV Scale Leptogenesis in B-L Model with Alternative Cosmologies*, *Phys. Lett. B* **725**, 361 (2013), [[arXiv:1205.1503 \[hep-ph\]](#)].
16. N. Okada and O. Seto, *Thermal leptogenesis in brane world cosmology*, *Phys. Rev. D* **73**, 063505 (2006), [[hep-ph/0507279](#)].
17. M. C. Bento, R. Gonzalez Felipe and N. M. C. Santos, *Aspects of thermal leptogenesis in braneworld cosmology*, *Phys. Rev. D* **73**, 023506 (2006), [[hep-ph/0508213](#)].
18. G. Panotopoulos, *Gravitino dark matter in brane-world cosmology*, *JCAP* **0705**, 016 (2007), [[hep-ph/0701233](#)].

18 *H. Abedi, A.M.Abbassi, S.Bahamonde*

19. N. Okada and O. Seto, *Gravitino dark matter from increased thermal relic particles*, *Phys. Rev. D* **77**, 123505 (2008), [arXiv:0710.0449 [hep-ph]].
20. J. U. Kang and G. Panotopoulos, *Dark matter in supersymmetric models with axino LSP in Randall-Sundrum II brane model*, *JHEP* **0805**, 036 (2008), [arXiv:0805.0535 [hep-ph]].
21. W. L. Guo and X. Zhang, *Constraints on Dark Matter Annihilation Cross Section in Scenarios of Brane-World and Quintessence*, *Phys. Rev. D* **79**, 115023 (2009), [arXiv:0904.2451 [hep-ph]].
22. S. Bailly, *Gravitino dark matter and the lithium primordial abundance within a pre-BBN modified expansion*, *JCAP* **1103**, 022 (2011), [arXiv:1008.2858 [hep-ph]].
23. M. T. Meehan and I. B. Whittingham, *Asymmetric dark matter in braneworld cosmology*, *JCAP* **1406**, 018 (2014), [arXiv:1403.6934 [astro-ph.CO]].
24. H. Abedi and A. M. Abbassi, *Primordial perturbations in multi-scalar Inflation*, *JCAP* **1707**, no. 07, 049 (2017), [arXiv:1606.05894 [gr-qc]].
25. H. Abedi and A. M. Abbassi, *Isocurvature perturbations during two-field inflation and reheating*, *Gen. Rel. Grav.* **51**, no. 2, 31 (2019).
26. E. Ramirez and A. R. Liddle, *Inflationary slow-roll formalism and perturbations in the Randall - Sundrum Type II brane world*, *Phys. Rev. D* **69**, 083522 (2004), [astro-ph/0309608].
27. Ø. Grøn, *Predictions of Spectral Parameters by Several Inflationary Universe Models in Light of the Planck Results*, *Universe* **4**, no. 2, 15 (2018).
28. R. M. Hawkins and J. E. Lidsey, *The inflationary energy scale in brane world cosmology*, *Phys. Rev. D* **68**, 083505 (2003), [astro-ph/0306311].
29. E. Ramirez and A. R. Liddle, *Braneworld flow equations*, *Phys. Rev. D* **71**, 027303 (2005), [astro-ph/0412556].
30. G. Calcagni, A.R. Liddle, E. Ramirez, *Flow equations in generalized braneworld scenarios*, *Phys. Rev. D* **72**, 043513 (2005), [astro-ph/0506558].
31. R. Easther and J. T. Giblin, *The Hubble slow roll expansion for multi field inflation*, *Phys. Rev. D* **72**, 103505 (2005), [astro-ph/0505033].
32. M. Spalinski, *New Solutions of the Inflationary Flow Equations*, *JCAP* **0708**, 016 (2007), [arXiv:0706.2503 [astro-ph]].
33. N. Okada and S. Okada, *Simple inflationary models in GaussBonnet brane-world cosmology*, *Class. Quant. Grav.* **33**, no. 12, 125034 (2016), [arXiv:1412.8466 [hep-ph]].
34. G. Calcagni, S. Kuroyanagi, J. Ohashi and S. Tsujikawa, *Strong Planck constraints on braneworld and non-commutative inflation*, *JCAP* **1403**, 052 (2014), [arXiv:1310.5186 [astro-ph.CO]].
35. D. S. Salopek and J. R. Bond, *Nonlinear evolution of long wavelength metric fluctuations in inflationary models*, *Phys. Rev. D* **42**, 3936 (1990).
36. W. H. Kinney, *Inflation: Flow, fixed points and observables to arbitrary order in slow roll*, *Phys. Rev. D* **66**, 083508 (2002), [astro-ph/0206032].
37. A. R. Liddle, *Inflationary flow equations*, *Phys. Rev. D* **68**, 103504 (2003), [astro-ph/0307286].
38. S. Bahamonde, C. G. Böhm, S. Carloni, E. J. Copeland, W. Fang and N. Tamanini, *Dynamical systems applied to cosmology: dark energy and modified gravity*, *Phys. Rept.* **775-777** (2018) 1 [arXiv:1712.03107 [gr-qc]].
39. R. Maartens, D. Wands, B. A. Bassett and I. P.C. Heard, *Chaotic inflation on the brane*, *Phys. Rev. D* **62**, 041301(R) (2000), [hep-ph/9912464].
40. D. Langlois, R. Maartens and D. Wands, *Gravitational waves from inflation on the brane*, *Phys. Lett. B* **489**, 259 (2000), [hep-th/0006007].
41. Y. Akrami *et al.* [Planck Collaboration], *Planck 2018 results. X. Constraints on in-*

*Hubble inflation in RSII model* 19

*flation*, [arXiv:1807.06211 \[astro-ph.CO\]](#).

42. B. Wang and E. Abdalla, *Plausible upper limit on the number of e-foldings*, [Phys. Rev. D](#) **69**, 104014 (2004), [[hep-th/0308145](#)].